Beam aperture modifier and beam deflector using gradient-index photonic crystals

Mengqian Lu,[1] Bala Krishna Juluri,[1] Sz-Chin Steven Lin,[1] Brian Kiraly,[1] Tieyu Gao,[2,a)] and Tony Jun Huang[1,b)]
[1]*Department of Engineering Science and Mechanics, The Pennsylvania State University, University Park, Pennsylvania 16802, USA*
[2]*School of Energy and Power Engineering, Xi'an Jiaotong University, Xi'an, Shaanxi 710049, China*

(Received 19 December 2009; accepted 7 September 2010; published online 17 November 2010)

We designed and simulated a beam aperture modifier and a beam deflector using two-dimensional parabolic gradient-index (GRIN) photonic crystals (PCs). The GRIN PCs are composed of dielectric columns with graded radii along the direction transverse to propagation. Both finite-difference time-domain methods and gradient optics analytical solutions were used to characterize the change in beam width and propagation direction. Multifunctional GRIN PCs combining both beam aperture modification and beam deflection were also designed and simulated. These GRIN PC based designs can be used as optical connectors and bidirectional waveguide couplers in applications such as miniaturized photonic integrated circuits. © *2010 American Institute of Physics*.
[doi:10.1063/1.3499630]

I. INTRODUCTION

Photonic crystals (PCs) are periodically engineered dielectric structures that can control the propagation of light analogous to the way solid crystals control the movement of electrons.[1–5] Incident light within specific frequency ranges, known as photonic bandgaps, are prohibited by the PCs due to Bragg reflection.[6–11] An efficient PC waveguide can, therefore, be obtained by simply introducing straight or bent line defects to the PC structures, making use of their low radiative loss within their bandgap.[12–17] Recent studies on PCs have demonstrated that negative refraction can also be obtained via the high crystal anisotropy of these artificially left-handed structures.[18–21] Because of their ability to control the propagation of electromagnetic waves and their compatibility with conventional micromachining techniques, PCs are promising candidates to assist the development of integrated photonic circuits and on-chip optical processing.[22–46]

The versatility of PCs in controlling light propagation can be further enhanced by introducing the concept of gradient-index (GRIN).[47–58] A conventional GRIN medium is characterized by a gradual variation in refractive index along the direction transverse to light propagation. Within the GRIN medium, light bends gradually toward higher refractive index per Snell's law, resulting in superior control over the propagation of light that cannot be achieved by an ordinary lens.[59–63] A GRIN PC can be considered as a discretized medium wherein each layer has an independent refractive index. Different refractive indices can be realized by locally adjusting the constitutive parameters of the PC, such as lattice spacing, dielectric index of fillers, or filling factors. Recently, effective focusing and collimation of waves has been achieved by GRIN PCs with linear or parabolic varying indices.[50–56] Furthermore, Centeno *et al.*[57,58] showed that wavelength-scale mirage and superbending effects can be obtained by GRIN PCs.

In this letter, we report our investigations using parabolic GRIN PCs to achieve both beam aperture modification and beam deflection. Beam aperture modification refers to changing the width of the incoming collimated radiation within the PC to a desired value. Beam deflection refers to changing the direction of an incident beam, which is similar to a specular reflection. To achieve these two functions (beam aperture modification and beam deflection), we have designed PCs composed of free-standing dielectric columns that are graded in radius perpendicular to the propagation. In our approach, a beam aperture modifier was achieved by combining two parabolic GRIN PCs with different gradient coefficients [Fig. 1(a)], and the beam deflector was realized by using one GRIN PC [Fig. 1(b)]. We used finite-difference time-domain (FDTD) methods to simulate the electromagnetic wave propagation through the PCs.[63] Our results indicate that the output width of the beam aperture modifier can be controlled by changing the ratio of gradient coefficients. The results also indicate that the output beam angle from the beam deflector can be controlled by changing the length of the PCs. We supplemented the simulations with analytical solutions based on Gaussian optics; this provides simple yet effective means to determine the expected beam width and angle for various input parameters. The comparison between the analytical solutions and the FDTD indicate that the results from these two approaches match well with each other.

II. BEAM APERTURE MODIFIER

The GRIN PCs used in our investigation are composed of a square array of silicon dioxide columns ($\varepsilon=2.5$) in air with a fixed lattice spacing, a. For a column-radius changing from $0.05a$ to $0.45a$ in increments of $0.05a$, we calculated the dispersion relations by considering a single unit cell with

a)Electronic mail: sunmoon@mail.xjtu.edu.cn.
b)Electronic mail: junhuang@psu.edu.

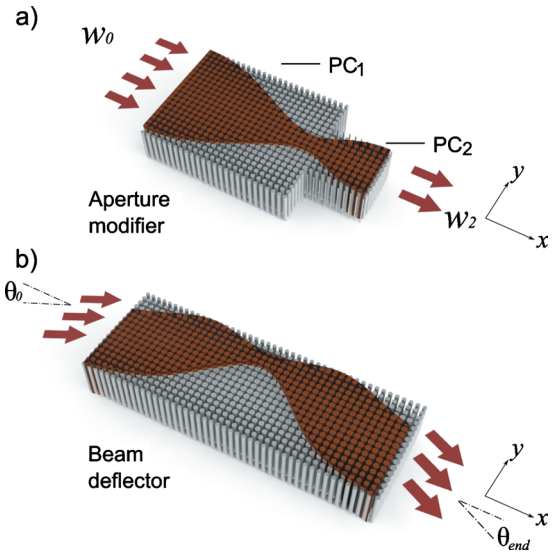

FIG. 1. (Color online) Schematic of (a) a beam aperture modifier and (b) a beam deflector based on GRIN PCs. The radii of the dielectric columns change transversely to the light propagation direction, forming parabolic GRIN PCs.

Bloch periodic boundary conditions in a 2D FDTD simulation.[63] Harmonic inversions of time signals were used to extract the frequency modes. Figure 2(a) shows the dispersion relations along ΓX orientation in wave vector space. The effective refractive index of the PCs can be obtained by the relationship $N_g = c/[\nabla_k \omega(k)]$, where c is the light velocity in vacuum, ω is the angular frequency, and k is the wave vector. Thus the change in N_g as a function of radius can be obtained once an operating frequency is fixed. Figure 2(b) shows the N_g-r/a relation at normalized frequency of 0.18 (if lattice constant $a=280$ nm, then the working wavelength is 1.55 μm).

As shown in Fig. 1(a), our beam aperture modifier consists of two parabolic GRIN PCs, PC_1 and PC_2, with different width and gradient coefficients. For normalized frequencies below 0.28, the equal-frequency contours for different r/a are nearly circular with anisotropic ratios ($r_a = N_{g\Gamma X}/N_{g\Gamma M}$) less than 1.02. Therefore, the PCs used in this work can be approximated as isotropic media (Figs. S1 and S2 in Ref. 66). The parabolically varying refractive indices in both PCs are given by the function, $N^2(y) = N_0^2(1-\alpha^2 y^2)$, where $N_0 = 1.406$ is the refractive index along the center axis (x axis) of the PC, y is the transverse distance to x axis in the unit of lattice constant a, and α is the gradient coefficient. There are 31 rows in PC_1 and 11 in PC_2, making the y range $[-10a, 10a]$ and $[-5a, 5a]$ in PC_1 and PC_2, respectively. Gradient coefficients $\alpha_1 = 0.0512$ and $\alpha_2 = 0.1367$ were chosen for PC_1 and PC_2, respectively, and radii values for the required distribution of refractive indices were then calculated according to the fitting curve shown in Fig. 2(b). In Fig. 2(c), we plot the effective refractive index and radius distributions in the proposed beam aperture modifier.

We further used a FDTD method to simulate the electromagnetic wave propagation throughout the GRIN PCs. According to Gaussian optics, in a parabolic GRIN medium, it takes a length of $\pi/(2\alpha)$ for an input Gaussian beam-source to focus or for a point-source to collimate.[60,64] In this case, the beam width is expected to achieve a minimum value after it goes through PC_1. Then the beam diverges through PC_2 until its width reaches a maximum value. Therefore, the lengths of the PCs were set to be $\pi/(2\alpha)$ ($l_1 = 31a$ for PC_1 and $l_2 = 11a$ for PC_2). A Gaussian beam of width $20a$ is located $1a$ in front of PC_1 and is centered at the x axis as the source. The magnetic field is confined in the x-y plane. The structure is surrounded by a perfectly matched layer (PML) of a thickness of $2a$.

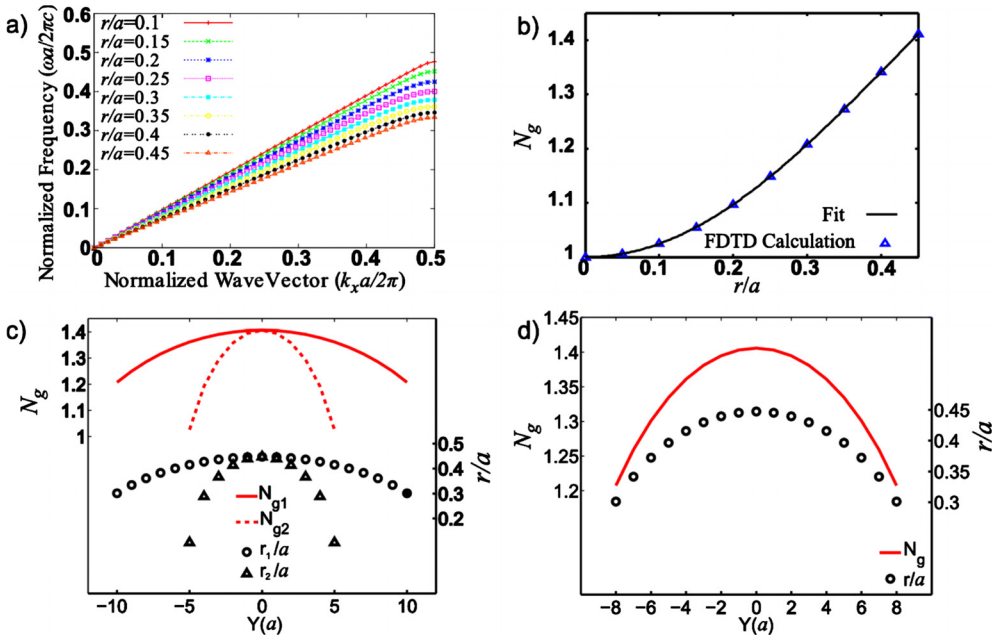

FIG. 2. (Color online) (a) Dispersion relations of PCs with different radii. (b) Variation in N_g with radii at a normalized frequency of 0.18 obtained from FDTD calculation (dots) and fit to the data (solid line). Refractive indices (solid lines) and radii (dots) distribution of (c) beam aperture modifier and (d) beam deflector.

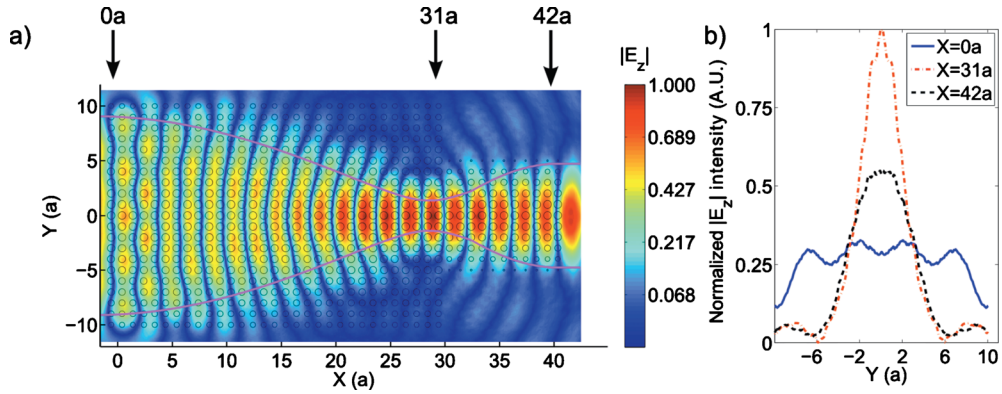

FIG. 3. (Color online) (a) FDTD simulation of the electric field in the beam aperture modifier. The line shows the beam trajectory derived from analytical expression. (b) Normalized electric field intensity distribution of the beam aperture modifier at $x=0a$, $x=31a$, and $x=42a$.

Figure 3(a) shows the FDTD-simulated steady-state electric field. As expected, the incident light focused first at the end of PC_1 and diverged again throughout PC_2 with a different beam width. The aperture ratio, $v=w_2/w_0$, is used to quantify the beam aperture modification, where w_2 and w_0 are the full widths at half maximum of the incident and transmitted light. The normalized electric intensity distribution at $x=0a$, $x=31a$, and $x=42a$ are shown in Fig. 3(b). According to the electric intensity distribution at $x=0a$ and $x=42a$, an aperture ratio of $v=0.3896$ is obtained.

We have also obtained analytical expressions of the beam trajectory and the beam width [as shown in Fig. 3(a)]. When the waist of the light beam is located at the input face of the GRIN PCs and the curvature radius of the beam profile at the input face is close to infinity ($R_0 \to \infty$), the beam width $[2w(x)]$ of the light propagating in the parabolic GRIN medium is described by:[61]

$$2w(x) = 2w_0 \sqrt{\cos^2 \alpha x + \frac{\sin^2 \alpha x \lambda^2}{\alpha^2 \pi^2 N_0^2 w_0^4}}, \tag{1}$$

where $2w_0$ is the beam width of the Gaussian beam source and λ is the normalized wavelength. The curvature radius $R(x)$ of the beam profile is determined by the following equation:[61]

$$\frac{1}{R(x)} = \frac{n_0 \sin \alpha x \cos \alpha x}{\cos^2 \alpha x + \frac{\sin^2 \alpha x \lambda^2}{\alpha^2 \pi^2 N_0^2 w_0^4}} \left(\frac{\lambda^2}{\alpha \pi^2 N_0^2 w_0^4} - \alpha \right). \tag{2}$$

When the light enters PC_2, the curvature radius is not infinite so the beam width in PC_2 cannot be calculated using Eq. (1). The equation in this case is:[61]

$$2w(x) = 2w_1 \sqrt{\left(\frac{\sin \alpha x}{\alpha N_0 R_1} + \cos \alpha x \right)^2 + \frac{\sin^2 \alpha x \lambda^2}{\alpha^2 \pi^2 N_0^2 w_1^4}}, \tag{3}$$

where R_1 is the curvature radius of the beam at the input face of PC_2 and $2w_1$ is the beam width at the input face of PC_2, which can be calculated by using Eqs. (1) and (2). Analytical Eqs. (1)–(3) give the theoretically calculated ratio $v_a = \alpha_1/\alpha_2 = (0.0512/0.1367) = 0.3745$. This value is only 5% different from the aperture ratio of the FDTD simulation (0.3896). This small deviation is likely caused by the fact that the PC cannot form a continuously parabolic gradient index profile, whereas a perfectly parabolic gradient index distribution is assumed in the calculation. Even though the device is designed at a normalized frequency of 0.18, it can achieve beam aperture modification for normalized frequencies between 0.135 and 0.28 (Fig. S3 in Ref. 66).

We can further enhance the beam aperture modification by enlarging the difference between α_1 and α_2. The value of α_2 can be enlarged by narrowing PC_2. Through changing the ratio α_1/α_2, we can modify the output beam width. The ratio α_1/α_2 can also be written in the form $\sqrt{[(N_0^2-N_1^2)\cdot Y_2^2]/[(N_0^2-N_2^2)\cdot Y_1^2]}$, where Y_1 and Y_2 are the width of PC_1 and PC_2, and N_1 and N_2 are the smallest refractive indices of PC_1 and PC_2, respectively. In a design where $N_0=1.406$, $N_1=1.229$, $N_2=1.025$, $Y_1=31a$, and $Y_2=11a$, we can achieve an aperture ratio as small as 0.15 based on the FDTD simulated results.

III. BEAM DEFLECTOR

In the design of the beam deflector, the number of rows is set to be 17, making the y range $[-8a, 8a]$. The gradient coefficient of the beam deflector is $\alpha=0.06406$. The index and radii distribution is shown in Fig. 2(d). The total length of the beam deflector is $l=48a$. During light propagation, the propagation direction will be refracted while the beam focuses and then diverges to its original width. In the FDTD simulation, the Gaussian beam of width $10a$ is located $8a$ in front of the PCs centered at $y=-3a$. The incident angle is 15°.

Additional equations are needed for analytical calculation of the beam path when the source light enters at an incident angle. The trajectory of the beam in a parabolic GRIN medium at any x value is determined by the incident position, y_0, the incident angle, θ_0, the coefficient of gradient, α, and the x value, as described by:[65]

$$y(x) = y_0 \cos \alpha x + \frac{\theta_0}{\alpha} \sin \alpha x, \tag{4}$$

According to Eq. (4), the slope of the trajectory, which is the tangent of the beam inclination angle, is predicted by the following equation:

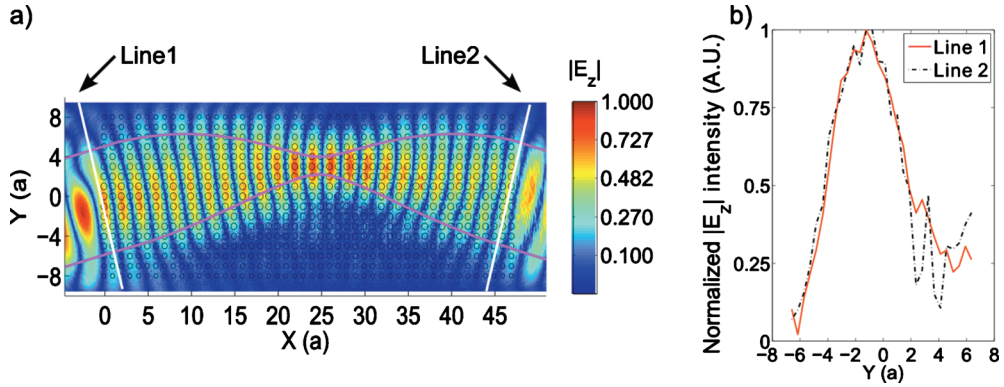

FIG. 4. (Color online) (a) FDTD simulation of the electric field in the beam deflector. The line shows the beam trajectory derived from analytical expression. (b) Normalized electric field intensity distribution of the beam deflector along line 1 and line 2.

$$\tan\,\theta(x) = \frac{dy}{dx} = -\,y_0\alpha\,\sin\,\alpha x + \theta_0\,\cos\,\alpha x, \tag{5}$$

Figure 4(a) indicates that GRIN PC can successfully be used to bend the light propagation direction. To quantify the bending effect, emergent angle θ_{end} was defined as the angle between the emergent light propagation direction and the x axis. Emergent light propagation direction was defined as the direction normal to the cross-section in which the transmitted beam had a normalized intensity distribution most similar to that of the incident beam. θ_{end} was calculated to be $-15.1°$, indicating that the light was deflected by 30.1°. Figure 4(b) shows that before (line 1) and after (line 2) the deflection, the normalized intensity distribution remains nearly identical. The beam deflector can maintain the deflection performance for normalized frequencies between 0.135 and 0.28 (Fig. S4 in Ref. 66).

The emergent angle can also be calculated theoretically using Eq. (5). In this case, the length is π/α, so the $\theta_{\text{end\_a}} = -\theta_0 = -15°$. By using different lengths of the beam deflector, according to Eq. (5), we can also obtain different "refraction angles." For instance, the PC can be a deflector if the length is $(2n\pi+\pi)/\alpha$ (here n can be any positive integer), which means $\theta_{\text{end\_a}} = -\theta_0$. If the length is $2n\pi/\alpha$, then $\theta_{\text{end\_a}} = \theta_0$, which means that the light propagation direction stays the same while the light is shifted along the length of PC.

IV. MULTIFUNCTIONAL GRIN PC

Since both beam aperture modification and beam deflection are obtained by using parabolic GRIN PCs, we can combine these two designs to achieve multifunctional PCs with both functions operating simultaneously. Using the beam source employed in the beam deflection and the PCs for beam aperture modification, we simulated the combination effect using the FDTD method [Fig. 5(a)]. The normalized electric intensity distribution of the incident beam and the emergent beam shown in Fig. 5(b) indicate that this multifunctional GRIN PC structure can change the beam width and the propagation direction simultaneously. However, there are some limitations in this design. Because the width of PC_2 is smaller than that of PC_1, if the incident light beam is too wide or the incident angle is too large, some of the light will propagate outside the PCs, leading to radiative loss. For example, in the design shown in Fig. 5, when the incident angle is enlarged to 25° or greater and the incident beam width is $14a$ or greater, there will be significant radiative loss. This multifunctional GRIN PCs operates for normalized frequencies between 0.153 and 0.28 (Fig. S5 in Ref. 66).

V. SUMMARY

We have designed a beam aperture modifier and a beam deflector using parabolic GRIN PCs. The performance of these GRIN PC-based devices was simulated and analyzed through both FDTD-based computational methods and gra-

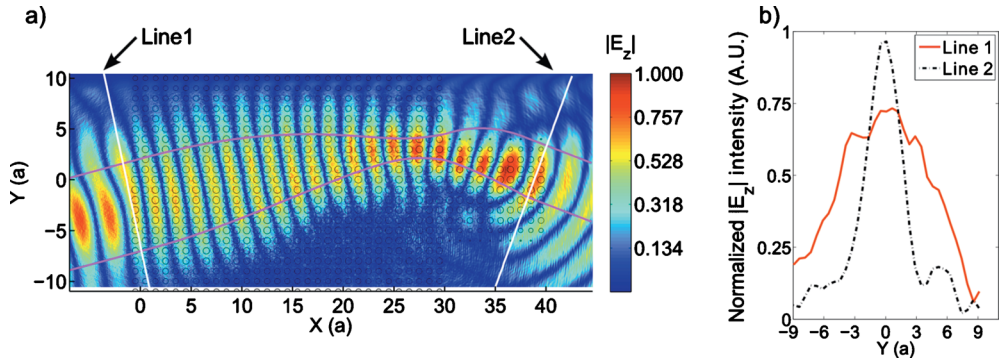

FIG. 5. (Color online) (a) FDTD simulation of the electric field in the multifunctional PCs. The line shows the beam trajectory derived from analytical expression. (b) Normalized electric field intensity distribution of the multifunctional PCs along line 1 and line 2.

dient optics-based analytical solutions. We have also designed a multifunctional GRIN PC combining both functions (beam aperture modification and beam deflection). Compared with the conventional approaches, the GRIN PC-based beam aperture modifier and beam deflector described here can be conveniently fabricated down to the micrometer scale. They can be used as connectors and bi-directional couplers and have promising potential in applications such as integrated photonic circuits and laboratory on a chip.

ACKNOWLEDGMENTS

We thank Joseph S. T. Smalley for helpful discussions. This work was supported by Air Force Office of Scientific Research (AFOSR), National Science Foundation (NSF), U.S. Department of Agriculture (USDA/NRI), and the Penn State Center for Nanoscale Science (MRSEC).

[1]E. Yablonovitch, Phys. Rev. Lett. **58**, 2059 (1987).
[2]S. John, Phys. Rev. Lett. **58**, 2486 (1987).
[3]P. L. Gourley, J. R. Wendt, G. A. Vawter, T. M. Brennan, and B. E. Hammons, Appl. Phys. Lett. **64**, 687 (1994).
[4]J. D. Joannopoulos, R. Meade, and J. N. Winn, *Photonic Crystals: Molding the Flow of Light* (Princeton University Press, Princeton, 1995).
[5]J. D. Joannopoulos, P. R. Villeneuve, and S. Fan, Nature (London) **386**, 143 (1997).
[6]T. F. Krauss, R. M. De La Rue, and S. Brand, Nature (London) **383**, 699 (1996).
[7]P. R. Villeneuve, S. Fan, and J. D. Joannopoulos, Phys. Rev. B **54**, 7837 (1996).
[8]S. Y. Lin, V. M. Hietala, L. Wang, and E. D. Jones, Opt. Lett. **21**, 1771 (1996).
[9]S. G. Johnson, S. Fan, P. R. Villeneuve, J. D. Joannopoulos, and L. A. Kolodziejski, Phys. Rev. B **60**, 5751 (1999).
[10]S. G. Johnson and J. D. Joannopoulos, Appl. Phys. Lett. **77**, 3490 (2000).
[11]I. V. Minin, O. V. Minin, Y. R. Triandaphilov, and V. V. Kotlyar, Prog. Electromagn. Res. B. **7**, 257 (2008).
[12]A. Mekis, J. C. Chen, I. Kurland, S. Fan, P. R. Villeneuve, and J. D. Joannopoulos, Phys. Rev. Lett. **77**, 3787 (1996).
[13]A. Yariv, Y. Xu, R. K. Lee, and A. Scherer, Opt. Lett. **24**, 711 (1999).
[14]M. Bayindir, B. Temelkuran, and E. Ozbay, Phys. Rev. Lett. **84**, 2140 (2000).
[15]S. G. Johnson, P. R. Villeneuve, S. Fan, and J. D. Joannopoulos, Phys. Rev. B **62**, 8212 (2000).
[16]M. Loncar, T. Doll, J. Vuckovic, and A. Scherer, J. Lightwave Technol. **18**, 1402 (2000).
[17]M. Augustin, H. Fuchs, D. Schelle, E. Kley, S. Nolte, A. Tunnermann, R. Iliew, C. Etrich, U. Peschel, and F. Ledereraugustin, Opt. Express **11**, 3284 (2003).
[18]R. A. Shelby, D. R. Smith, and S. Schultz, Science **292**, 77 (2001).
[19]M. Notomi, Phys. Rev. B **62**, 10696 (2000).
[20]E. Cubukcu, K. Aydin, E. Ozbay, S. Foteinopoulou, and C. M. Soukoulis, Nature (London) **423**, 604 (2003).
[21]J. Shi, S. S. Lin, and T. J. Huang, Appl. Phys. Lett. **92**, 111901 (2008).
[22]D. W. Prather, S. Shi, J. Murakowski, G. J. Schneider, A. Sharkawy, C. Chen, B. Miao, and R. Martin, J. Phys. D: Appl. Phys. **40**, 2635 (2007).
[23]M. Zickar, W. Noell, C. Marxer, and N. De Rooij, Opt. Express **14**, 4237 (2006).
[24]A. R. McGurn, Phys. Rev. B **61**, 13235 (2000).
[25]H. Benisty, J. Lourtioz, A. Chelnokov, S. Combrié, and X. Checoury, Proc. IEEE **94**, 997 (2006).
[26]L. Eldada, Opt. Eng. **40**, 1165 (2001).
[27]T. Liu, A. R. Zakharian, R. Rathnakumar, M. Fai, J. V. Moloney, and M. Mansuripur, Proc. SPIE **5380**, 430 (2004).
[28]X. Yu and S. Fang, Appl. Phys. Lett. **83**, 3251 (2003).
[29]H. Kosaka, T. Kawashinma, A. Tomita, M. Notomi, T. Tamamura, T. Sato, and S. Kawakami, Appl. Phys. Lett. **74**, 1212 (1999).
[30]D. W. Prather, S. Shi, D. M. Pustai, C. Chen, S. Venkataraman, A. Sharekawy, G. J. Schneider, and J. Murakowski, Opt. Lett. **29**, 50 (2004).
[31]Y. Fink, J. N. Winn, S. Fan, C. Chen, J. Michel, J. D. Joannopoulos, and E. L. Thomas, Science **282**, 1679 (1998).
[32]A. F. Matthews, S. K. Morrison, and Y. S. Kivshar, Opt. Commun. **279**, 313 (2007).
[33]Y. Zheng, B. K. Juluri, X. Mao, T. R. Walker, and T. J. Huang, J. Appl. Phys. **103**, 014308 (2008).
[34]Y. Zheng, T. J. Huang, A. Y. Desai, S. J. Wang, L. K. Tan, H. Gao, and A. C. H. Huan, Appl. Phys. Lett. **90**, 18 (2007).
[35]Y. B. Zheng, Y.-W. Yang, L. Jensen, L. Fang, B. K. Juluri, A. H. Flood, P. S. Weiss, J. F. Stoddart, and T. J. Huang, Nano Lett. **9**, 819 (2009).
[36]Y. B. Zheng, L. Jensen, W. Yan, T. R. Walker, B. K. Juluri, L. Jensen, and T. J. Huang, J. Phys. Chem. C **113**, 7019 (2009).
[37]V. K. S. Hsiao, J. R. Waldeisen, Y. Zheng, P. F. Lloyd, T. J. Bunning, and T. J. Huang, J. Mater. Chem. **17**, 4896 (2007).
[38]X. Mao, J. R. Waldeisen, and T. J. Huang, Lab Chip **7**, 1260 (2007).
[39]X. Mao, J. R. Waldeisen, B. K. Juluri, and T. J. Huang, Lab Chip **7**, 1303 (2007).
[40]J. Shi, X. Mao, D. Ahmed, A. Colletti, and T. J. Huang, Lab Chip **8**, 221 (2008).
[41]X. Mao, S.-C. S. Lin, C. Dong, and T. J. Huang, Lab Chip **9**, 1583 (2009).
[42]J. Shi, D. Ahmed, X. Mao, S.-C. S. Lin, and T. J. Huang, Lab Chip **9**, 2890 (2009).
[43]J. Shi, H. Huang, Z. Stratton, A. Lawit, Y. Huang, and T. J. Huang, Lab Chip **9**, 3354 (2009).
[44]B. K. Juluri, M. Lu, Y. B. Zheng, L. Jensen, and T. J. Huang, J. Phys. Chem. C **113**, 18499 (2009).
[45]D. Ahmed, X. Mao, B. K. Juluri, and T. J. Huang, Microfluid. Nanofluid. **7**, 727 (2009).
[46]D. Ahmed, X. Mao, J. Shi, B. K. Juluri, and T. J. Huang, Lab Chip **9**, 2738 (2009).
[47]L. Wu, L. Li, and J. Zhang, Phys. Rev. A **78**, 013838 (2008).
[48]F. Hudelist, R. Buczynski, A. J. Waddie, and M. R. Taghizadeh, Opt. Express **17**, 3255 (2009).
[49]H. Kurt and D. S. Citrin, IEEE Photonics Technol. Lett. **19**, 1532 (2007).
[50]H. Kurt and D. S. Citrin, Opt. Express **15**, 1240 (2007).
[51]H. Kurt, E. Colak, O. Cakmak, H. Caglayan, and E. Ozbay, Appl. Phys. Lett. **93**, 171108 (2008).
[52]F. S. Roux and I. D. Leon, Phys. Rev. B **74**, 113103 (2006).
[53]S.-C. S. Lin, B. R. Tittmann, J.-H. Sun, T.-T. Wu, and T. J. Huang, J. Phys. D: Appl. Phys. **42**, 185502 (2009).
[54]B. C. Gupta and Z. Ye, Phys. Rev. B **67**, 153109 (2003).
[55]S.-C. S. Lin, T. J. Huang, J.-H. Sun, and T.-T. Wu, Phys. Rev. B **79**, 094302 (2009).
[56]B. K. Juluri, S.-C. S. Lin, T. R. Walker, L. Jensen, and T. J. Huang, Opt. Express **17**, 2997 (2009).
[57]E. Centeno and D. Cassagne, Opt. Lett. **30**, 2278 (2005).
[58]E. Centeno, D. Cassagne, and J. Albert, Phys. Rev. B **73**, 235119 (2006).
[59]H. Kogelnik, Appl. Opt. **4**, 1562 (1965).
[60]W. J. Tomlinson, Appl. Opt. **19**, 1127 (1980).
[61]C. Gómez-Reino, M. V. Perez, and C. Bao, *Gradient-index Optics: Fundamentals and Applications* (Springer, Berlin, 2002).
[62]A. O. Pinchuk and G. C. Schatz, J. Opt. Soc. Am. A **24**, A39 (2007).
[63]X. Mao, S.-C. S. Lin, M. I. Lapsley, J. Shi, B. K. Juluri, and T. J. Huang, Lab Chip **9**, 2050 (2009).
[64]A. Taflove, *Computational Electrodynamics: The Finite-Difference Time-Domain Method* (Artech House, Norwood, 2000).
[65]B. E. A. Saleh and M. C. Teich, *Fundamentals of Photonics* (Wiley, New York, 1991).
[66]See supplementary material at http://dx.doi.org/10.1063/1.3499630 for details regarding isotropic characterization and effect of frequency on the beam guiding performance.